Inorg. Chem. **2007**, *46*, 610–612

Cyanide-Bridged Fe(III)–Mn(III) Chain with Metamagnetic Properties and Significant Magnetic Anisotropy

Shi Wang,*,† Marilena Ferbinteanu,*,†,§ and Masahiro Yamashita†,‡

Department of Chemistry, Graduate School of Science, Tohoku University, Aramaki, Aoba-ku, Sendai 980-8578, Japan, and CREST, Japan Science and Technology Agency (JST), Honcho, Kawaguchi-shi, Saitama 332-0012, Japan

Received September 6, 2006

The assembling of $[Mn(5\text{-}MeOsalen)(H_2O)]^+$ and $[(Tp)Fe(CN)_3]^-$ affords the one-dimensional zigzag chain $[(Tp)Fe(CN)_3Mn(5\text{-}MeOsalen)\cdot 2CH_3OH]_n$ [**1**; $Tp^- =$ hydrotris(pyrazolyl)borate and $5\text{-}MeOsalen^{2-} = N,N'$-ethylenebis(5-methoxysalicylideneiminate)]. The corroborated experimental and ab initio data indicate ferromagnetic Fe(III)–Mn(III) couplings and $D < 0$ anisotropy on Mn(III). The field-induced metamagnetic behavior is due to interchain effects.

The structural variety,[1] the outlined synthetic strategies,[2] and the challenging properties,[3] such as high-T_C magnetism, photomagnetism, and pressure tuning of magnetization, promote the cyanide-bridged complexes as top candidates for the design of new materials. Beyond the potential technical applications, the cyanide-bridged-based single-molecule magnets[4] and single-chain magnets (SCMs)[5] are interesting for the structural rationalization of spin and anisotropy effects.[6] A key factor is the negative D axial term in the zero-field-splitting (ZFS) Hamiltonian. The previous obtaining of a SCM[7a] based on the pronounced magnetic anisotropy of salicylideneiminate (salen)-type Mn(III) complexes[7b] and the ferromagnetic Fe(III)−CN−Mn(III) coupling[7c] prompted us for the design and investigation of similar extended systems. The presented compound, $[(Tp)Fe^{III}(CN)_3Mn^{III}(5\text{-}MeOsalen)\cdot 2CH_3OH]_n$ (**1**), has negative D and positive J parameters. Even not having SCM features offers an interesting magnetostructural case.

Compound **1** was obtained as dark-brown crystals by the reaction of $(Bu_4N)[(Tp)Fe(CN)_3]$[8] ($Bu_4N^+ =$ tetrabutylammonium) and $[Mn(5\text{-}MeOsalen)(H_2O)](PF_6)$[9] in a 1:1 molar ratio in methanol. Crystallography data[10] reveal the one-dimensional (1D) neutral polymer $[(Tp)Fe^{III}(CN)_3Mn^{III}(5\text{-}$

* To whom correspondence should be addressed. E-mail: swang@agnus.chem.tohoku.ac.jp (S.W.), marilena@agnus.chem.tohoku.ac.jp (M.F.).
† Tohoku University.
§ Permanent address: Department of Inorganic Chemistry, University of Bucharest, Dumbrava Rosie 23, Bucharest 70254, Romania. E-mail: mcimpoesu@yahoo.com.
‡ CREST, JST.

(1) (a) Dunbar, K. R.; Heintz, R. A. *Prog. Inorg. Chem.* **1997**, *45*, 283. (b) Verdaguer, M.; Bleuzen, A.; Marvaud, V.; Vaissermann, J.; Seuleiman, M.; Desplanches, C.; Scuiller, A.; Train, C.; Garde, R.; Gelly, G.; Lomenech, C.; Rosenman, I.; Veillet, P.; Cartier, C.; Villain, F. *Coord. Chem. Rev.* **1999**, *190*−*192*, 1023. (c) Ohkoshi, S.; Tokoro, H.; Hashimoto, K. *Coord. Chem. Rev.* **2005**, *249*, 1830.

(2) (a) Lescouezec, R.; Toma, L. M.; Vaissermann, J.; Verdaguer, M.; Delgado, F. S.; Ruiz-Perez, C.; Lloret, F.; Julve, M. *Coord. Chem. Rev.* **2005**, *249*, 2691 and references cited therein. (b) Beltran, L. M. C.; Long, J. R. *Acc. Chem. Res.* **2005**, *38*, 325 and references cited therein.

(3) (a) Ferlay, S.; Mallah, T.; Ouahés, R.; Veillet, P.; Verdaguer, M. *Nature* **1995**, *378*, 701. (b) Sato, O.; Iyoda, T.; Fujishima, A.; Hashimoto, K. *Science* **1996**, *272*, 704. (c) Egan, L.; Kamenev, K.; Papanikolaou, D.; Takabayashi, Y.; Margadonna, S. *J. Am. Chem. Soc.* **2006**, *128*, 6034.

(4) (a) Sokol, J. J.; Hee, A. G.; Long, J. R. *J. Am. Chem. Soc.* **2002**, *124*, 7656. (b) Berlinguette, C. P.; Vaughn, D.; Cañada-Vilalta, C.; Galán-Mascarós, J. R.; Dunbar, K. R. *Angew. Chem., Int. Ed.* **2003**, *42*, 1523. (c) Choi, H. J.; Sokol, J. J.; Long, J. R. *Inorg. Chem.* **2004**, *43*, 1606. (d) Song, Y.; Zhang, P.; Ren, X.-M.; Shen, X.-F.; Li, Y.-Z.; You, X.-Z. *J. Am. Chem. Soc.* **2005**, *127*, 3708. (e) Miyasaka, H.; Takahashi, H.; Madanbashi, T.; Sugiura, K.; Clérac, R.; Nojiri, H. *Inorg. Chem.* **2005**, *44*, 5969. (f) Li, D.; Parkin, S.; Wang, G.; Yee, G. T.; Clérac, R.; Wernsdorfer, W.; Holmes, S. M. *J. Am. Chem. Soc.* **2006**, *128*, 4214.

(5) (a) Lescouëzec, R.; Vaissermann, J.; Ruiz-Pérez, C.; Lloret, F.; Carrasco, R.; Julve, M.; Verdaguer, M.; Dromzee, Y.; Gatteschi, D.; Wernsdorfer, W. *Angew. Chem., Int. Ed.* **2003**, *42*, 1483. (b) Toma, L. M.; Lescouëzec, R.; Lloret, F.; Julve, M.; Vaissermann, J.; Verdaguer, M. *Chem. Commun.* **2003**, 1850. (c) Toma, L.; Lescouëzec, R.; Pasán, J.; Ruiz-Pérez, C.; Vaissermann, J.; Cano, J.; Carrasco, R.; Wernsdorfer, W.; Lloret, F.; Julve, M. *J. Am. Chem. Soc.* **2006**, *128*, 4842.

(6) Weihe, H.; Güdel, H. U. *Comments Inorg. Chem.* **2000**, *22*, 75.

(7) (a) Ferbinteanu, M.; Miyasaka, H.; Wernsdorfer, W.; Nakata, K.; Sugiura, K.; Yamashita, M.; Coulon, C.; Clérac, R. *J. Am. Chem. Soc.* **2005**, *127*, 3090. (b) Miyasaka, H.; Ieda, H.; Matsumoto, N.; Re, N.; Crescenzi, R.; Floriani, C. *Inorg. Chem.* **1998**, *37*, 255. (c) Re, N.; Gallo, E.; Floriani, C.; Miyasaka, H.; Matsumoto, N. *Inorg. Chem.* **1996**, *35*, 6004.

(8) (a) Lescouëzec, R.; Vaissermann, J.; Lloret, F.; Julve, M.; Verdaguer, M. *Inorg. Chem.* **2002**, *41*, 5943. (b) Wang, S.; Zuo, J.-L.; Zhou, H.-C.; Choi, H. J.; Ke, Y.; Long, J. R.; You, X.-Z. *Angew. Chem., Int. Ed.* **2004**, *43*, 5940. (c) Wang, S.; Zuo, J.-L.; Gao, S.; Song, Y.; Zhou, H.-C.; Zhang, Y.-Z.; You, X.-Z. *J. Am. Chem. Soc.* **2004**, *126*, 8900. (d) Wang, S.; Zuo, J.-L.; Zhou, H.-C.; Song, Y.; Gao, S.; You, X.-Z. *Eur. J. Inorg. Chem.* **2004**, 3681. (e) Wang, C.-F.; Zuo, J.-L.; Bartlett, B. M.; Song, Y.; Long, J. R.; You, X.-Z. *J. Am. Chem. Soc.* **2006**, *128*, 7162.

(9) Kennedy, B. J.; Murray, K. S. *Inorg. Chem.* **1985**, *24*, 1552.

(10) Crystal and structure refinement parameters for **1**: $C_{32}H_{36}BN_{11}O_6MnFe$, fw = 792.30, $T = 100$ K, monoclinic, space group $P2_1/n$, $Z = 4$, $a = 11.9236(15)$ Å, $b = 11.8939(15)$ Å, $c = 25.680(3)$ Å, $\beta = 100.805(3)°$, $V = 3577.3(8)$ Å^3, $D_{calc} = 1.471$ g cm^{-3}, 35 306 reflections collected, 8248 unique, R1 = 0.0490, wR2 = 0.1440 [$I > 2\sigma(I)$].

10.1021/ic061681n CCC: $37.00
Published on Web 01/11/2007

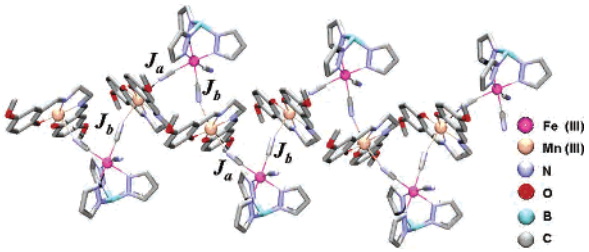

Figure 1. Structure of the 1D chain for **1** with magnetic exchanges as indicated. H atoms and methanol molecules are omitted for clarity.

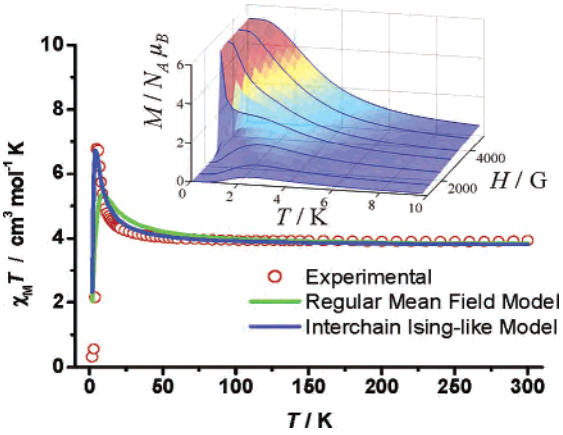

Figure 2. $\chi_M T$ vs T for **1**. Solids lines: fit with different interchain models. Inset: dependence of relative magnetization M vs H and T computed using the Ising-like interchain interaction model, parallel with the experimental pattern (Figure S4 in the Supporting Information).

MeOsalen)]$_n$, with free solvate methanol into the crystal spaces (Figures 1 and S1 in the Supporting Information). The zigzag pattern is determined by the cis topology of bridges emerging from $[TpFe(CN)_3]^-$. The Mn ion is six-coordinated in an elongated octahedral geometry (formally, a Jahn−Teller distortion). The equatorial plane is occupied by N_2O_2 donor atoms of 5-MeOsalen [Mn−N(1) = 1.986(2) Å, Mn−N(2) = 1.980(2) Å, Mn−O(1) = 1.873(2) Å, and Mn−O(2) = 1.863(2) Å]. The chain shows two alternating types of Fe−C≡N−Mn bridges, labeled here a and b, closely similar in bond lengths, e.g., $(Mn-N)_a$ = 2.364(2) Å and $(Mn-N)_b$ = 2.320(2) Å, but having different bond and dihedral angles, like $(C\equiv N-Mn)_a$ = 161.7(2)° vs $(C\equiv N-Mn)_b$ = 151.1(2)° and $(Fe-C\equiv N-Mn)_a$ = 23.7° vs $(Fe-C\equiv N-Mn)_b$ = 158.2°. Such geometry factors determine quantitative differentiation in the exchange parameters. The Fe−C bond lengths [1.920(3)−1.933(3) Å] are in the range known for other low-spin Fe(III) complexes.[8] The Fe−C≡N angles for both terminal [174.5(3)°] and bridging [174.4(3) and 175.7(3)°] cyanide groups depart slightly from linearity.

The dc magnetic measurements were carried out on a polycrystalline sample in the range of 1.8−300 K at an external field of 1000 G. For magnetization measurements, the sample was restrained in eicosane to prevent torquing. The $\chi_M T$ curve, with a ferromagnetic main pattern and an antiferromagnetic trend at lower T, is shown in Figure 2. At low temperatures, **1** exhibits peculiar magnetic properties. As shown in Figure S4 in the Supporting Information, χ_M reaches a maximum at 4.8 K for low fields, which broadens

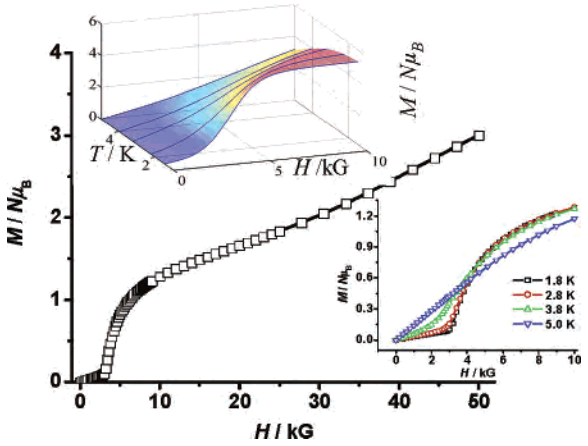

Figure 3. Field dependence of the magnetization for **1** at 1.8 K. Lower inset: Experimental magnetization isotherms at temperatures as indicated. Upper inset: magnetization isotherms simulated by the model.

as H increases and disappears for H > 3500 G, proving a field-induced transition from an antiferromagnetic to a ferromagnetic ground state.[11] ac susceptibility measurements at different frequencies (500, 1000, and 1400 Hz) in a zero dc field show a zero out-of-phase component (χ'') and the in-phase one (χ') practically coincident to the χ_M curve. No frequency-dependent behavior was observed. The transition temperature (T_N) can be estimated as 4.4 K by the maximum of $d(\chi' T)/dT$ at 1000 Hz. The field dependence of the magnetization up to 50 kG was measured at various temperatures (1.8, 2.8, 3.8, and 5.0 K; Figure 3). As the temperature is reduced, the isotherms become increasing sigmoidal. The value of the critical field (H_C) is 3600 G (the inflection point in the inset of Figure 3). The curve at 1.8 K has the behavior expected for a metamagnet with a large anisotropy. Up to 50 kG, the maximum recorded magnetization, ~3 $N\mu_B$, is not reached, yet the saturation value, $g_{Mn}S_{Mn} + g_{Fe}S_{Fe} \sim 5\ N\mu_B$, shows, however, a firmly increasing slope.

The alternating topology is described with J_a and J_b Mn(III)−Fe(III) coupling parameters (Figure 1). The anisotropy of Mn(III) is accounted for by the D axial ZFS term. Under periodicity conditions, the infinite chain is equivalent to a ring. The finite alternating $\{MnFe\}_n$ rings can be cut in two ways, through J_a or J_b contacts. At sufficiently large n, the magnetism of the ring and open chains converge identically. Taking an average of $\chi_M T$ computed for the ring and the two chains, one achieves a smooth trend to the simulation of the infinite chain. We afforded the fit for the $n = 3$ case, with larger systems being prohibitive in iterative procedures (the number of spin states is 10^n). A mean-field parameter ($zJ < 0$) was tentatively considered to explain the decrease of $\chi_M T$ in the 1.8−4 K range. However, the fit with g = 2.11, J_a = 1.93 cm^{-1}, J_b = 1.83 cm^{-1}, zJ = −0.19 cm^{-1}, and D = −2.41 cm^{-1} does not show a good curve match. Thorough improvement attempts revealed the intrinsic incapacity of the mean field to account well for the case. The mean field works with a $-zJ \cdot S_z^i \langle S_z^i \rangle$ Hamiltonian

(11) (a) Re, N.; Gallo, E.; Floriani, C.; Miyasaka, H.; Matsumoto, N. *Inorg. Chem.* **1996**, *35*, 6004. (b) Carlin, R. L. *Magnetochemistry*; Springer-Verlag: New York, 1986.

defined as an Ising-like term between spin projections of each i state and the averaged spin projection.[12] It does not introduce new states, amending only the free system ones. For two interacting chains, with N states each, the full Heisenberg or Ising coupling would produce N^2 levels, prohibitively multiplying the number of states, beyond the necessary phenomenology of the weak interaction. The compromise between standard mean-field and regular interchain Ising models is reached by conceiving Ising-like terms acting only between degenerate states of the two chains. Then, instead of N^2 states, we introduce $2N$ ones for the resonant interaction of chain levels, ascribed by the $-zJ\cdot S_z^i(1)\, S_z^i(2)$ term, with (1) and (2) labeling the chains. The coupling parameter in the new Hamiltonian is conventionally kept in the zJ notation. It is intuitive that the resonant effects between degenerate levels play a higher effective role than the $S_z^i(1)\, S_z^j(2)$ cross terms.

With this model, $\chi_M T$ can be fitted in an excellent manner, giving $g = 2.11$, $J_a = 1.66$ cm^{-1}, $J_b = 1.21$ cm^{-1}, $zJ = -0.038$ cm^{-1}, and $D = -0.95$ cm^{-1}. D is in the usual range (-1 to -4 cm^{-1}) for Schiff base complexes.[9] The considered model also reproduces the patterns of M vs H and T in a semiquantitative manner (the upper insets in Figures 2 and 3). Possibly, the $\chi_M T$ fit is nonunique, on the basis of compensation effects usual in multiparametric cases. A multibranch fit of $\chi_M T$ and M to the experimental data is taken as the goal of a further work. Confined to the actual form, the model enables the understanding of the lattice magnetism in **1**. The steep decrease in $\chi_M T$ at low temperature is due to the interchain antiferromagnetic coupling. The interchain Ising-like resonant interaction model, which tacitly incorporates the chain anisotropy, explains the observed magnetization effects. Taking two chains for the effective modeling of the supramolecular coupling, we have for each state i of the individual chain a $2|zJ|(S_z^i)^2$ gap between four collective states grouped in two degenerate pairs, one set originating from the $\{(+S_z^i, +S_z^i), (-S_z^i, -S_z^i)\}$ chain couples and another set from the $\{(+S_z^i, -S_z^i), (-S_z^i, +S_z^i)\}$ ones. The field-tuned crossing of the ground-state levels (with the above degeneracy pattern) determines the recorded phase transition (Scheme S4 in the Supporting Information).

The ab initio calculations were taken as a complement in the magnetostructural analysis.[13] The broken-symmetry density functional theory (DFT) calculations[14] performed on corresponding a and b {FeMn} dimer moieties taken from the experimental geometry lead to $J_a = 2.4$ cm^{-1} and $J_b = 1.7$ cm^{-1} estimations, which are consistent with the range and sign of the experimental fit values.

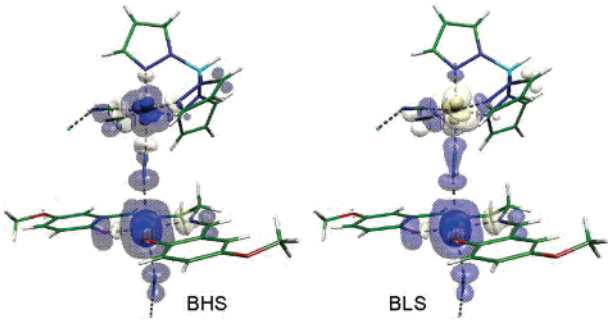

Figure 4. Spin-density maps from broken-symmetry DFT calculations for the a dimer sequence (α in blue; β in light yellow). The solid surfaces correspond to 0.05 e Å^{-3} and the transparent ones to 0.002 e Å^{-3} isovalues.

The spin populations along the cyanide bridge show the following patterns: $Mn^{4\alpha}N^{\delta\alpha}C^{\delta'\beta}Fe^{1\alpha}$ for the broken-symmetry high-spin (BHS) case and $Mn^{4\alpha}N^{\delta\alpha}C^{\delta'\alpha}Fe^{1\beta}$ for the broken-symmetry low-spin (BLS) case (Figure 4 and spin populations in the Supporting Information). A spin-polarization effect takes place at the Fe−C contact, which can be presented as a cause of ferromagnetism. The ferromagnetic interaction can also be understood by observing that the magnetic orbital on Fe(III) has a dπ nature (from t_{2g} parentage) that falls into an orthongonality relationship with the σ (d_{z^2}) type magnetic orbital oriented along the CN−Mn−NC mean axes. Because of the Mn(III) d_{z^2} type molecular orbital's relative interaction propensity toward the Fe(III) center, this ferromagnetic channel dominates the overall coupling.

In summary, we firmly conclude the ferromagnetic nature of the two Fe(III)−Mn(III) couplings, with certain differentiation due to the differences in bridging angles. The antiferromagnetic interchain coupling causes the metamagnetic behavior of **1** with loss of magnetization relaxation effects. Further synthetic and interpretation works on related systems are underway.

Acknowledgment. S.W. and M.F. acknowledge the Japan Society for the Promotion of Science for postdoctoral fellowships [P06351 (S.W.) and P04390 (M.F.)]. S.W. is thankful for the COE program and M.F. for CNCSIS/RO-886/2005. We are grateful to Dr. F. Cimpoesu for programming support. We thank Prof. H. Miyasaka, Dr. T. Kajiwara, and Dr. S. Takaishi for discussions.

Supporting Information Available: X-ray crystallographic file (CIF) for **1**, additional experimental, structural, magnetic and computational details. The material is available free of charge via the Internet at http://pubs.acs.org.

IC061681N

(12) Kahn, O. *Molecular Magnetism*; Wiley-VCH: New York, 1993; p 131. The mean-field susceptibility is $\chi_{MF} = \chi[1 - zJ\chi/(N_A g^2 \mu_B^2)]^{-1}$, where χ is the reference molar susceptibility, N_A Avogadro's number, μ_B the Bohr magneton, and g the Lande factor.

(13) Bencini, A.; Dei, A.; Sangregorio, C.; Totti, F.; Vaz, M. G. F. *Inorg. Chem.* **2003**, *42*, 8065.

(14) (a) Noodleman, L. *J. Chem. Phys.* **1981**, *74*, 5737. (b) Bencini, A.; Totti, F.; Daul, C. A.; Doclo, K.; Fantucci, P.; Barone, V. *Inorg. Chem.* **1997**, *36*, 5022. (c) Mitani, M.; Mori, H.; Takano, Y.; Yamaki, D.; Yoshioka, Y.; Yamaguchi, K. *J. Chem. Phys.* **2000**, *113*, 4035.